




In silico and NMR studies on pharmaceutical compounds with therapeutic action against Myasthenia Gravis

Errikos Petsas^{a*}, Eleftherios Massios^{a*}, Nikitas Georgiou^a, Antigoni Cheilari^b, Panagiotis Konstantinos Papadimitriou^a, Margarita Georgia Kakava^c, Ektoros Vasileios Apostolou^a, Ioannis Angelonidis^d, Nikolaos Eleftheriadis^d, Demeter Tzeli^{e,f}  and Thomas Mavromoustakos^a

^aLaboratory of Organic Chemistry, Department of Chemistry, National and Kapodistrian University of Athens, Athens, Greece; ^bDepartment of Pharmacognosy and Natural Products Chemistry, Faculty of Pharmacy, National and Kapodistrian University of Athens, Athens, Greece; ^cLaboratory of Organic Chemistry and Biochemistry, Department of Chemistry, University of Patras, Patras, Greece; ^dLaboratory of Biophysical Chemistry, Department of Chemistry, University of Crete, Heraklion, Greece; ^eLaboratory of Physical Chemistry, Department of Chemistry, National and Kapodistrian University of Athens, Athens, Greece; ^fTheoretical and Physical Chemistry Institute, National Hellenic Research Foundation, Athens, Greece

ABSTRACT

Myasthenia Gravis, a chronic autoimmune disease, is primarily treated with acetylcholinesterase inhibitors. However, these drugs are not specific, and their mechanism of action against the disease has not been elucidated. They have a propensity to act on different targets, and their therapeutic action is symptomatic. For this reason, we have studied the interactions of commercially available drugs against Myasthenia Gravis to various enzyme targets to examine if there is any selectivity in their action and possibly to reveal any potential use for other diseases. In particular, the Computational Chemistry programs, AutoDock and Maestro, were used to assess the binding of azathioprine, prednisone, and pyridostigmine to different classes of enzymes, such as: cyclooxygenases (COX-1, COX-2), monoamine oxidases (MAO-A, MAO-B), angiotensin receptors (AT1, AT2), and lipoxygenases (LOX-1, 5-LOX). Molecular Dynamics simulations were employed to further analyze the stability and interactions of the most effective compounds. Using *in silico* platforms it was found that these drugs are not toxic, they do not produce unwanted adverse effects, and that pyridostigmine seems to be the best compound according to the ADME results. Additionally, Saturation Transfer Difference NMR experiments were carried out and confirmed the binding of azathioprine to LOX-5 at both the molecular and atomic levels. The *in vitro* evaluation of azathioprine and prednisone also revealed important inhibition of human 15-LOX-1 over general lipoxygenase activity. Finally, it was found that these drugs have potential for use in various biological and pharmacological applications such as CNS drugs.

ARTICLE HISTORY

Received 11 March 2025
Accepted 6 July 2025

KEYWORDS

Myasthenia Gravis;
azathioprine; prednisone;
pyridostigmine; DFT; STD;
docking; *in vitro*

1. Introduction

Myasthenia gravis (MG) (Schrodinger, 2013) is a chronic autoimmune disorder that affects neuromuscular transmission, leading to muscle weakness and fatigue, particularly after physical exertion. This condition impacts approximately 50 to 200 individuals per million (Jorgensen et al., 1996). The underlying cause of MG is an immune system attack on key proteins involved in neuromuscular junction communication, specifically through the production of autoantibodies that block signal transmission between nerves and muscles (Georgiou et al., 2023).

There are two main forms of MG: ocular myasthenia gravis (OMG), which accounts for about 15% of cases, and generalized myasthenia gravis (gMG), which represents the remaining 85% (Schrodinger, 2013). Clinical research indicates that most MG patients initially experience ocular symptoms, such as ptosis and diplopia. Moreover, around half of those with ocular symptoms develop generalized MG

CONTACT Thomas Mavromoustakos  tmavrom@chem.uoa.gr

*These authors contributed equally to this work.

within two years. If the disease remains confined to ocular muscles beyond this period, it is likely to stay localized (Imtiaz et al., 2021). Typically MG appears before the age of 50 and is more frequently observed in women (Essmann et al., 1995; Martyna et al., 1994).

The global prevalence of autoimmune MG is estimated to range from 40 to 180 cases per million, with an annual incidence of 4 to 12 cases per million. Recent data suggest an increasing prevalence and incidence, particularly for late-onset MG, which may be attributed to improved diagnostic methods, greater awareness, and an aging population. Additionally, advancements in treatment have contributed to lower mortality rates associated with MG (Georgiou et al., 2023; Humphreys et al., 1994; Lyman & Zuckerman, 2006; Schrodinger, 2013).

Although the exact mechanisms and triggers of MG are not fully understood, research has established that immune system dysfunction plays a key role. The disorder is primarily caused by autoantibodies targeting acetylcholine receptors (AChRs) on the postsynaptic membrane of neuromuscular junctions (Imtiaz et al., 2021). This attack reduces AChR levels, impairs neuromuscular transmission, and results in muscle weakness and fatigue. While MG has no definitive cure, several treatment options are available to manage symptoms effectively. Proper classification of patients into subgroups is essential for ensuring optimal therapeutic strategies (Essmann et al., 1995; Version, D.D.; Viegas et al., 2011).

Treatment for MG typically includes anticholinesterases, corticosteroids, immunosuppressants, and mycophenolate mofetil, along with urgent interventions for temporary symptom relief. Among the most commonly prescribed medications are azathioprine, pyridostigmine, and prednisone (Papaemmanouil et al., 2020; Vrontaki et al., 2015).

Azathioprine (AZA) (see the structure on Figure 1(a)) is widely used in the treatment of MG, rheumatoid arthritis (RA), and in preventing kidney transplant rejection. It acts as an immunosuppressant, helping to regulate the overactive immune response associated with these conditions. Azathioprine functions as an immunosuppressant by mimicking purine structures and disrupting DNA synthesis. It mainly targets rapidly dividing T and B lymphocytes by inhibiting the enzyme inosine monophosphate dehydrogenase. This action diminishes the immune system's activity against acetylcholine receptors (AChRs), thereby helping to control the autoimmune response associated with (MG) (Eleftheriadis et al., 2015, 2016a, 2016b; Louka et al., 2025; Spacho et al., 2024).

Prednisone (see structure in Figure 1(b)), an FDA-approved corticosteroid, is also frequently prescribed for MG and other inflammatory and autoimmune disorders. It reduces inflammation and modulates immune activity, thereby alleviating symptoms such as muscle weakness and fatigue. Prednisone is a corticosteroid that works by binding to glucocorticoid receptors, which results in the suppression of pro-inflammatory gene expression and the activation of genes involved in anti-inflammatory responses.

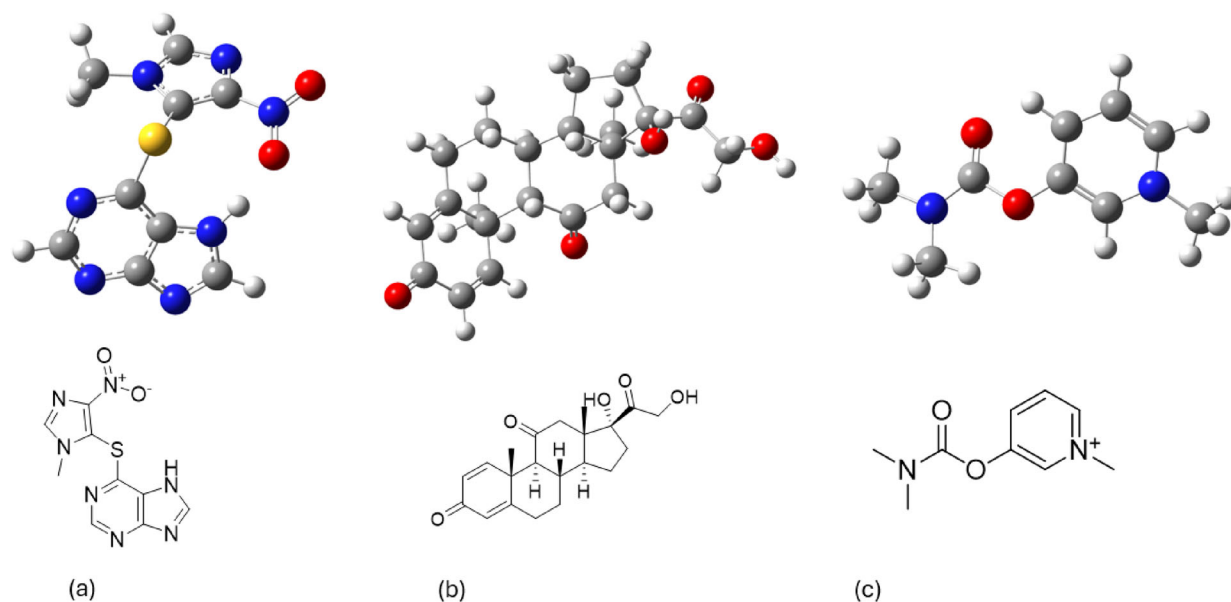


Figure 1. Optimized conformations of (a) azathioprine, (b) prednisone and (c) pyridostigmine.

This mechanism leads to a reduction in lymphocyte proliferation and cytokine release, ultimately lowering the production of autoantibodies targeting the acetylcholine receptor (AChR).

Pyridostigmine, (see the structure on [Figure 1\(c\)](#)) an acetylcholinesterase inhibitor, is the first-line treatment for most MG patients. Despite being the preferred symptomatic treatment, no randomized controlled trials have been conducted to formally assess its efficacy, and limited research exists on its perceived benefits from the patient's perspective (Louka et al., 2025). Furthermore, studies on the frequency of pyridostigmine's side effects remain scarce. Pyridostigmine is a reversible inhibitor of acetylcholinesterase that increases acetylcholine levels at the neuromuscular junction by preventing its degradation. This enhances neuromuscular signaling and provides symptomatic relief by offsetting the loss of functional acetylcholine receptors (AChRs) caused by autoantibodies.

Azathioprine, prednisone, and pyridostigmine each exhibit unique long-term characteristics that are relevant for clinical application. Azathioprine delivers prolonged immunosuppressive effects but is associated with potential adverse effects such as liver toxicity, bone marrow suppression, and an elevated risk of cancer. Prednisone is highly effective in the short term but poses notable long-term risks, including osteoporosis, metabolic disturbances, and generalized immunosuppression (Eleftheriadis et al., 2016a, 2016b). Pyridostigmine, on the other hand, is typically well tolerated during extended use, offering consistent symptomatic improvement without impacting disease progression. Evaluating their chronic toxicity and sustained effectiveness is essential for understanding their long-term safety and therapeutic value in treating chronic conditions.

The above information indicates that Myasthenia Gravis, a chronic autoimmune disease, which is primarily treated with acetylcholinesterase inhibitors, is not treated with specific drugs that show a selective mechanism of action but their therapeutic index is relied on symptomatic effects. For this reason, we have initiated studies on the interactions of the available drugs against Myasthenia Gravis to various enzyme targets to examine if there is any selectivity in their action. While MAO, COX, AT1 and LOX enzymes do not directly cause myasthenia gravis, they may influence the disease's pathophysiology through their roles in neurotransmitter metabolism and inflammatory processes. Altered neurotransmitter levels due to MAO activity, increased inflammation mediated by COX and LOX pathways, and the resulting immune responses could exacerbate the symptoms and progression of MG. Understanding these mechanisms may help in developing targeted therapies to manage the condition. Computational Chemistry programs, AutoDock and Maestro, were used to assess the binding of azathioprine, prednisone, and pyridostigmine to different classes of enzymes, such as: cyclooxygenases (COX-1, COX-2), monoamine oxidases (MAO-A, MAO-B), angiotensin receptors (AT1, AT2), and lipoxygenases (LOX-1, 5-LOX). Molecular Dynamics simulations analyzed the stability and interactions of the most effective compounds. Using *in silico* platforms their physical chemical properties, pharmacokinetics, pharmacodynamics and toxicity were studied here.

2. Materials and methods

2.1. Molecular binding

In-silico experiments were conducted using SwissTarget Prediction to forecast potential macromolecular targets for the studied drugs. The analysis identified 21 possible targets. To further explore drug-protein interactions, AutoDock 4, a tool that facilitates flexible molecular modeling, was used. This software allows specific protein side chains to be designated as flexible, making it easier to model dynamic interactions. This approach helped to simulate and understand the binding interactions between the enzyme and the drug, providing insights into the enzyme-binding complex.

2.2. Induced fit docking

AutoDock and Maestro (Schrödinger) utilize different algorithms and scoring functions to simulate molecular binding interactions. The difference between the two methods lies in the fact that when using AutoDock the metals are removed from the molecules under study and therefore they show different binding energy values. For this reason, Maestro software was used for the enzymes with metals in their

active center. The preparation of each molecular structure was carried out separately using the «Protein Preparation Wizard» application of the Maestro program from Schrödinger. The molecular structures of the enzymes studied are found deposited in the online database «Protein DataBank-PDB» as monomeric or polymeric structures and can be downloaded directly into the Maestro program. During molecular binding, the monomeric structure was used to speed up the results due to incorrect grid positioning by Maestro program on the dimeric structure of the protein. All the ligands were prepared from LigPrep. The geometries were optimized using MacroModel to relax the structures while maintaining proper chiralities at the chiral centers. The OPLS2005 force field was employed for minimization. All compounds underwent protonation state adjustments for physiological pH (~ 7.4). Hammett and Taft methods, alongside an ionization tool, were utilized to create chemically sensitive 3D models. The 3D structures of ligands were further minimized with MacroModel (Schrodinger, 2013) using water as the solvent and OPLS2005 (Jorgensen et al., 1996) as the force field, employing a conjugate gradient (CG) method with a threshold of 0.01 kcal/mol. The resulting minimized structure served as input for a mixed-torsional/low-sampling conformational search, preserving the original chirality. This search generated multiple conformers for each molecule, which were then energetically ranked. The most favorable conformation was selected as input for subsequent docking calculations (Georgiou et al., 2023).

2.3. Molecular dynamics

Molecular dynamics (Imtiaz et al., 2021) (MD) simulations were performed using SPC/E-modeled water molecules to solvate the drug-protein complex. To achieve neutralization, Na^+ and Cl^- ions were introduced until the salt concentration reached 0.150 M NaCl. The N-terminus of the protein was modified with an acetyl group, while the C-terminus remained uncapped as it plays a role in the protein's active site. Protein-ligand interactions were simulated using the OPLS2005 force field, with long-range electrostatics computed through the particle mesh Ewald (PME) (Essmann et al., 1995; Martyna et al., 1994) method, utilizing a grid spacing of 0.8 Å. Van der Waals and short-range electrostatic forces were smoothly truncated at a distance of 9.0 Å. The Nose-Hoover thermostat (Humphreys et al., 1994) regulated temperature, while the Martyna-Tobias-Klein method maintained pressure stability. Periodic boundary conditions were applied, and the simulation box dimensions were set at $(10.0 \times 10.0 \times 10.0)$ Å. For numerical integration (Lyman & Zuckerman, 2006), the multistep RESPA algorithm was employed, using an inner time step of 2 fs for bonded interactions and non-bonded interactions within a 9 Å cutoff, while a larger outer time step of 6.0 fs was applied to non-bonded interactions beyond this cutoff. The system underwent equilibration following Desmond's (Version, D.D.) standard protocol, beginning with Brownian dynamics relaxation in the NVT ensemble at 310 K, with solute heavy atoms constrained. This was followed by an additional relaxation phase in the NPT ensemble without constraints for 1.0 ns. The production phase of the MD simulation spanned 200 ns to ensure sufficient sampling of the molecule's binding behavior within the protein's cavity. Simulations were conducted on workstations with GPU-accelerated MD codes, and statistical analysis was performed by evaluating the RMSD convergence of the protein backbone $\text{C}\alpha$ atoms and the ligand's RMSD.

2.4. Saturation transfer difference (STD)

For STD experiments, the azathioprine NMR sample was prepared by first dissolving azathioprine in DMSO, then adding potassium phosphate buffer (pH 7.2) in D_2O , creating a total volume of 600 μL with a 20 mM buffer concentration and pH 7.2 in 99.9% D_2O . The concentration of azathioprine in the NMR tube (600 μL) was 1000 μM and 1 μM for the enzyme in the NMR tube (600 μL), resulting in a protein-ligand ratio of 1:1000. These samples were then subjected to STD experiments at 25 °C at 900 MHz spectrometer in the University of Utrecht (Papaemmanouil et al., 2020; Viegas et al., 2011; Vrontaki et al., 2015).

Regarding the STD NMR experiments of prednisone, the following procedure was followed: first, a stock solution was prepared by dissolving 11.68 mg of prednisone in 700 μL of DMSO-d_6 . From this solution, 2.5 μL were taken and added to an Eppendorf containing 50 μL D_2O , 435.5 μL phosphate buffer with pH = 7.15. Also it is added to the same Eppendorf a 10 μL of a solution of 5-LOX (MW = 78.500), 500 u, $C = 20.84$ mg/mL and 738.02 u/mL in 100 mM Tris, pH = 8, 5 mM EGTA, 1 mM CaCl_2 , 30% Glycerol.

This was stirred in a vortex apparatus, and 498 μL of the solution was transferred to 5 mm NMR tube. Finally, the spectra were obtained using a Bruker 500 MHz spectrometer installed at the Chemistry Department of the University of Athens.

2.5. ADMET calculations

The compounds were sketched in ChemDraw and they were converted into SMILES in order to be used in SwissADME, pKCSM and pro-TOX platforms. This was performed to identify the pharmacological and toxicological parameters of each compound.

2.6. Enzyme inhibition studies

The human 15-LOX-1 was expressed in BL21 (DE3) *E. coli* cells and the cell lysate was used for the activity assay, as described in the literature (Adamis et al., 2025; Eleftheriadis et al., 2015, 2016a, 2016b; Louka et al., 2025; Spacho et al., 2024). Lipoxidase from Glycine max (soybean) was purchased (L7395, Sigma-Aldrich). Each measurement was performed in triplicate, and all data were processed with Microsoft Excel Professional Plus 2021 and GraphPad Prism 9.0.0 software.

3. Results

3.1. Molecular binding

The molecular docking results between the compounds and the macromolecules are shown in Table 1.

The most favorable targets were found to be the 6FVZ (monoamine oxidase B MAO-B) and 2Z5X (monoamine oxidase A MAO-A), with values quite lower than -8 , indicating strong binding. Specifically, binding energy values lower than -8 kcal/mol indicate strong binding because such values are often considered significant in docking studies, depending on the target and docking protocol. Thus, these compounds can serve as potential leads for these targets. The interactions that developed upon binding of azathioprine and prednisone to the 6FVZ protein of the MAO-B enzyme are represented in Figures 2 and 3. In particular, a π - π stacking bond is observed between the imidazole ring and Tyr 326. Two hydrogen bonds are also formed. The nucleophilic nitrogen of the imidazole ring forms an H bond with a water molecule. This water molecule simultaneously forms an H bond with the amino acid Gln 206. The second bonding is between the -OH with Pro-102. As shown in Figure 3, in the case of prednisone we observe only the formation of H bonds with water molecules. Also, when comparing with known inhibitors of LOX, e.g. zileuton, the docking score is approximately -8 kcal/mol. According to the data in Table 1, prednisone binds stronger to 5-LOX (Georgiou et al., 2023). Moreover, if we compare the docking results with the known inhibitor of LOX, zileuton, it is observed that prednisone binds stronger than zileuton ($\Delta G = -8.56$ kcal/mol). For BChe, it is observed that the known inhibitor rivastigmine binds stronger than the studied drugs (Georgiou et al., 2023).

In Figures 4–6, the docking poses of the three drugs with common targets found using SwissADME are shown. Specifically, the targets were found from the SwissADME platform. The green spheres represent the hydrogen bonds and the yellow net represents π - π interactions.

As can be seen from Figures 4–6, each ligand binds to the same pocket in the active center. Furthermore, they interact with the same amino acids in most cases. Specifically, in Carbonic anhydrase VII arginine forms 4 hydrogen bonds with ARG168, HIS331, HIS412 and GLU411 and one π - π interaction with HIS412. In addition, prednisone forms 3 hydrogen bonds with GLU411, ASP327 and LYS328. Finally, pyridostigmine forms two hydrogen bonds with SER102 and ARG168. On the other hand, in carbonic anhydrase XII, azathioprine forms 4 hydrogen bonds with HIS119, THR200, HIS396 and HIS96 and one π - π interaction with HIS94. Moreover, prednisone forms 3 hydrogen bonds with THR200, THR199 and TRP5. Pyridostigmine forms 3 hydrogen bonds with HIS96, HIS94 and HIS119. Finally, in alkaline phosphatase, azathioprine forms 3 hydrogen bonds with HIS96, HIS119 and HIS94 and one π - π interaction with HIS96, while prednisone forms only one hydrogen bond with LEU198. Last but not least,

Table 1. Binding energies BE (kcal/mol) during molecular docking between (the compounds pyridostigmine, azathioprine and prednisone) and macromolecule targets.

	Binding energy (kcal/mol)
4EY7 (human acetylcholinesterase) (Cheung et al., 2012)	
Pyridostigmine	−6.04 ± 0.5
Azathioprine	−5.31 ± 0.5
Prednisone	−6.02 ± 0.5
5DYW (human butylcholinesterase) (Kořak et al., 2016)	
Pyridostigmine	−0.88 ± 0.5
Azathioprine	−0.74 ± 0.5
Prednisone	−1.04 ± 0.5
5UEN (human adenosine) (Glukhova et al., 2017)	
Pyridostigmine	−4.83 ± 0.5
Azathioprine	−6.55 ± 0.5
Prednisone	−8.63 ± 0.5
1YK8 (cathepsin k) (Barrett et al., 2005)	
Pyridostigmine	−4.46 ± 0.5
Azathioprine	−5.50 ± 0.5
Prednisone	−5.05 ± 0.5
4XIX (carbonic anhydrase cah3 from Chlamydomonas) (Benlloch et al., 2015)	
Pyridostigmine	−4.92 ± 0.5
Azathioprine	−6.16 ± 0.5
Prednisone	−5.97 ± 0.5
3D4N (dehydrogenase) (Julian et al., 2008)	
Pyridostigmine	−3.67 ± 0.5
Azathioprine	−4.68 ± 0.5
Prednisone	−7.38 ± 0.5
4UXJ (thymidine kinase) (Timm et al., 2015)	
Pyridostigmine	−6.33 ± 0.5
Azathioprine	−8.86 ± 0.5
Prednisone	−9.61 ± 0.5
5XR8 (cannabinoid CB1) (Hua et al., 2017)	
Pyridostigmine	−5.21 ± 0.5
Azathioprine	−6.48 ± 0.5
Prednisone	−10.4 ± 0.5
6KPF (cannabinoid) (Hua et al., 2020)	
Pyridostigmine	−5.11 ± 0.5
Azathioprine	−7.04 ± 0.5
Prednisone	−9.26 ± 0.5
6LU7 (sars-cov-2) (Jin et al., 2020)	
Pyridostigmine	−4.85 ± 0.5
Azathioprine	−6.26 ± 0.5
Prednisone	−8.31 ± 0.5
2Z5X (monoamine oxidase A MAO-A) (Son et al., 2008)	
Pyridostigmine	−4.33 ± 0.5
Azathioprine	−10.60 ± 0.5
Prednisone	−13.52 ± 0.5
6FVZ (monoamine oxidase B MAO-B) (Reis et al., 2018)	
Pyridostigmine	−4.58 ± 0.5
Azathioprine	−8.39 ± 0.5
Prednisone	−13.94 ± 0.5
3LN1 (cyclooxygenase-2 COX-2) (Wang et al., 2010)	
Pyridostigmine	−3.69 ± 0.5
Azathioprine	−7.52 ± 0.5
Prednisone	−12.24 ± 0.5
6D01 (AT1 antagonist) (Samara & Yang, 2018)	
Pyridostigmine	−3.71 ± 0.5
Azathioprine	−5.62 ± 0.5
Prednisone	−8.53 ± 0.5
6JOD (AT2 antagonist) (Asada et al., 2020)	
Pyridostigmine	−2.84 ± 0.5
Azathioprine	−5.07 ± 0.5
Prednisone	−6.45 ± 0.5
5T5V (LOX-1) (Offenbacher et al., 2017)	
Pyridostigmine	−3.97 ± 0.5
Azathioprine	−6.63 ± 0.5
Prednisone	
3O8Y (5-LOX) (Gilbert et al., 2011)	
Pyridostigmine	−5.54 ± 0.5
Azathioprine	−5.17 ± 0.5
Prednisone	−12.45 ± 0.5

(continued)

Table 1. Continued.

	Binding energy (kcal/mol)
1ALK (alkaline phosphatase tissue-nonspecific isozyme) (Kim & Wyckoff, 1991)	
Pyridostigmine	-3.73 ± 0.5
Azathioprine	-5.34 ± 0.5
Prednisone	-6.43 ± 0.5
1JD0 (carbonic anhydrase XII) (Whittington et al., 2001)	
Pyridostigmine	-4.85 ± 0.5
Azathioprine	-6.64 ± 0.5
Prednisone	-8.18 ± 0.5
6H37 (carbonic anhydrase VII) (Buemi et al., 2019)	
Pyridostigmine	-5.23 ± 0.5
Azathioprine	-6.54 ± 0.5
Prednisone	-7.32 ± 0.5
2POM (15-Lipoxygenase)	
Pyridostigmine	-3.60 ± 0.5
Azathioprine	-5.03 ± 0.5
Prednisone	-6.18 ± 0.5

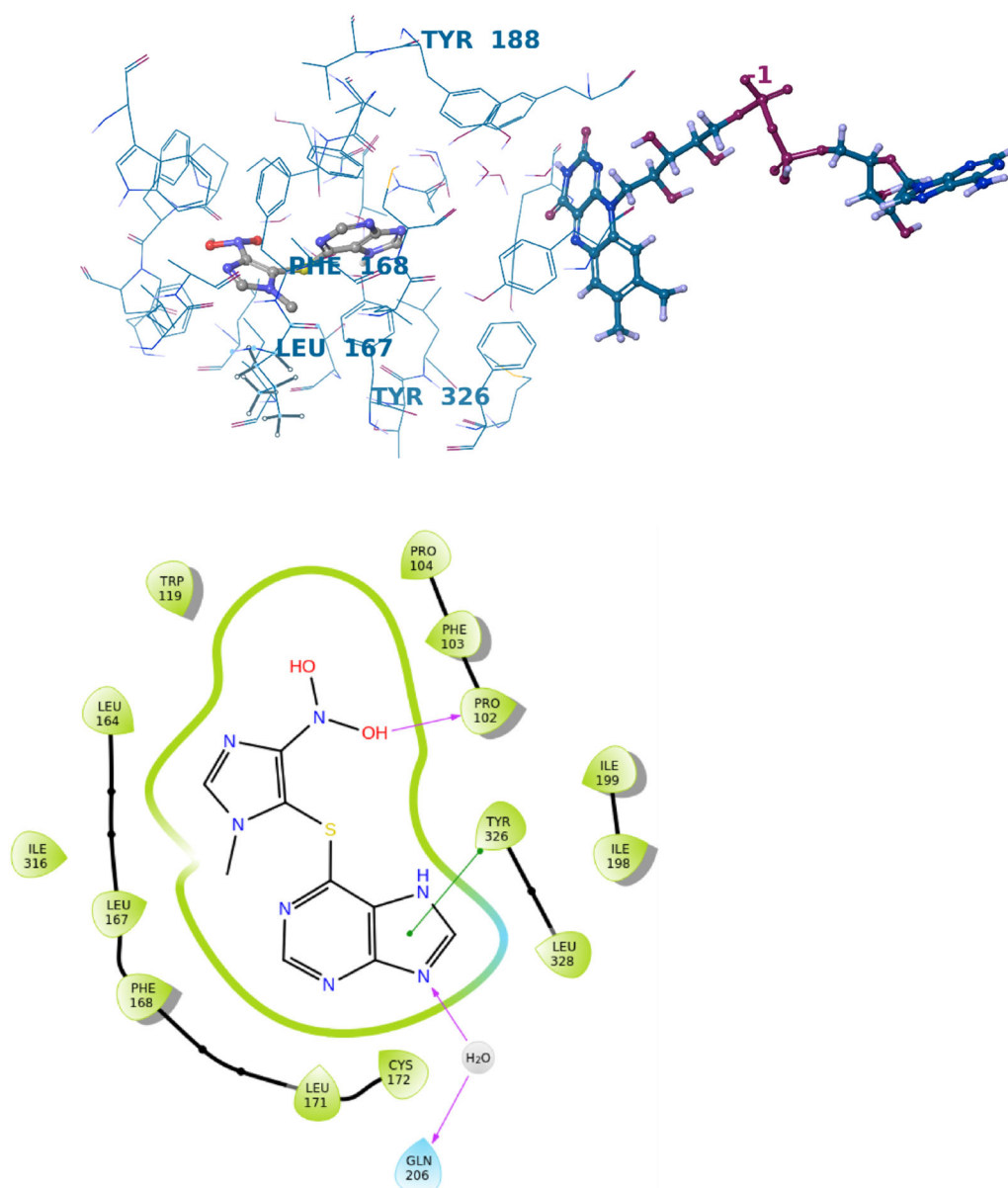


Figure 2. Azathioprine binding to the MAO-B enzyme in 2D and 3D representation.

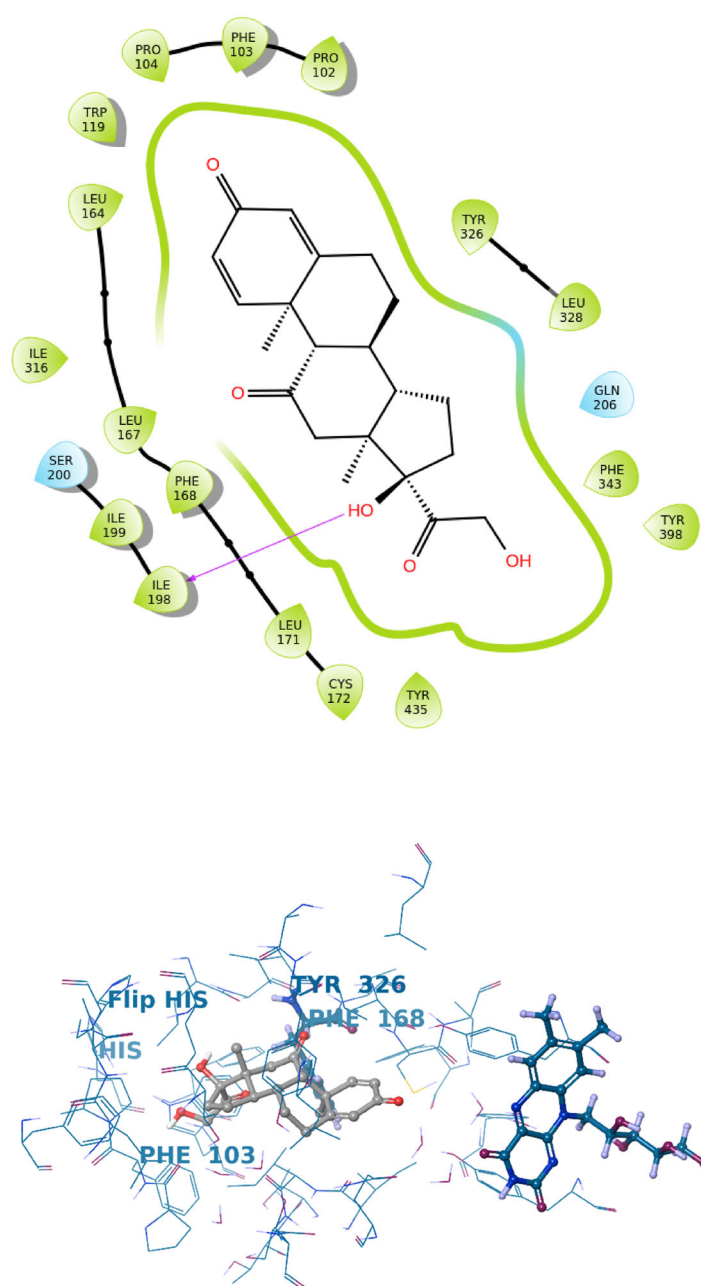


Figure 3. Prednisone binding to the MAO-B enzyme in 2D and 3D representation.

pyridostigmine forms 4 hydrogen bonds with HIS95, HIS94, HIS119 and THR199. All the interactions are shown in Table 2. As a result, these three drugs show a lack of selectivity.

The side effects of azathioprine (Chande et al., 2016) and prednisone (Schacke, 2002) vary. Specifically, some common side effects include weight gain, mood changes, fever, infections and skin rash. These side effects may have an impact on nervous system which is related with the MAO-B (Pasinetti, 1996) enzyme and also with inflammation which is related with COX-1 (Smith et al., 2000) enzyme. Specifically, prednisone has a broader and more direct impact on the nervous system, particularly in terms of mood changes, cognitive issues, and psychiatric symptoms like steroid psychosis. It can also cause insomnia, memory issues, and even increased intracranial pressure. Azathioprine is less likely to cause direct neurological side effects, but it may indirectly affect the nervous system through immune suppression, leading to infections that can involve the brain or nerves. In rare cases, it can lead to peripheral neuropathy due to bone marrow suppression. Both azathioprine and prednisone are used to treat inflammatory diseases but can lead to various side effects related to inflammation. Azathioprine is

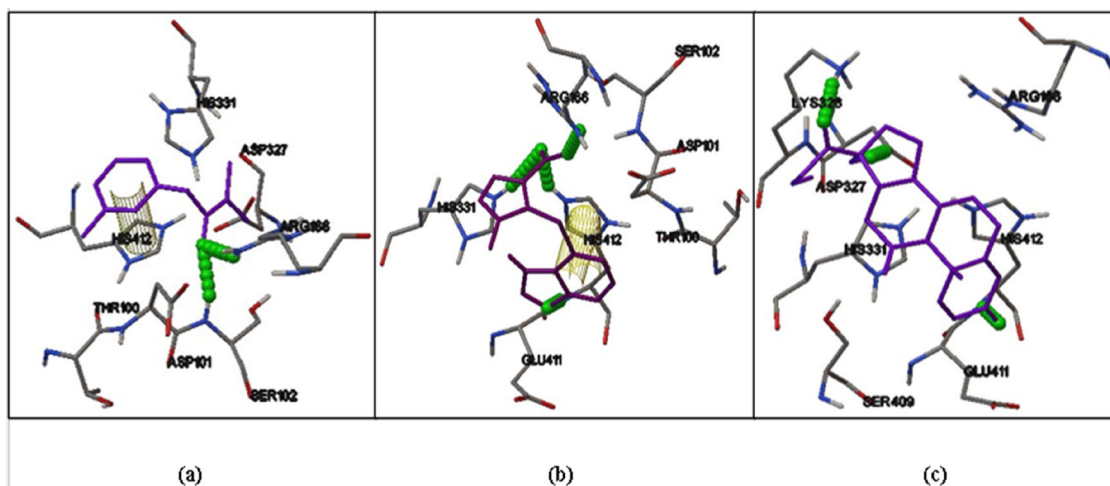


Figure 4. Interactions of pyridostigmine (a), azathioprine (b) and prednisone (c) with alkaline phosphatase, tissue-nonspecific isozyme (1ALK).

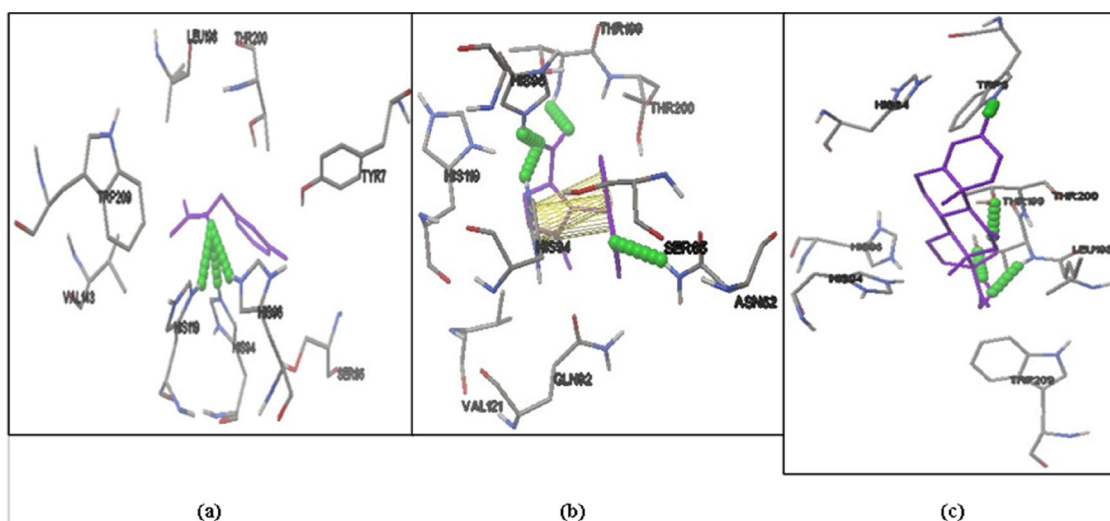


Figure 5. Interactions of pyridostigmine (a), azathioprine (b) and prednisone (c) with carbonic anhydrase XII (1JD0).

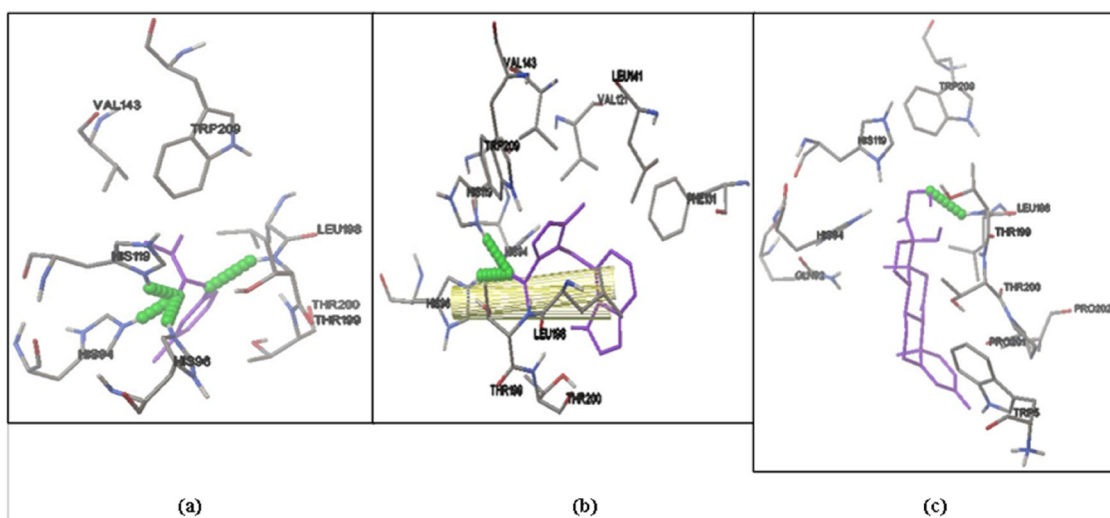


Figure 6. Interactions of pyridostigmine (a), azathioprine (b) and prednisone (c) with carbonic anhydrase VII (6H37).

Table 2. Interactions of the drugs with the common targets found using SwissADME platform.

Carbonic anhydrase VII	Hydrogen bonds	π - π interactions
Azathioprine	ARG168, HIS331, HIS412, GLU411	HIS412
Prednisone	GLU411, ASP327, LYS328	
Pyridostigmine	SER102, ARG168	
Carbonic anhydrase XII		
Azathioprine	HIS119, THR200, HIS396, HIS96	HIS94
Prednisone	THR200, THR199, TRP5	
Pyridostigmine	HIS96, HIS94, HIS119	
Alkaline phosphatase		
Azathioprine	HIS96, HIS119, HIS94	HIS96
Prednisone	LEU198	
Pyridostigmine	HIS95, HIS94, HIS119, THR199	

less likely to cause direct inflammatory side effects but can lead to inflammation of organs like the liver or pancreas in rare cases. Prednisone, while highly effective at reducing inflammation, has a more extensive range of side effects, and a higher risk of infections that can trigger inflammatory responses. From [Figures 2 and 3](#), it appears that azathioprine and prednisone bind to MAO-B in the same pocket. This could explain neurological symptoms, such as mood swings, insomnia, or psychosis, particularly in prednisone. Finally, from [Figures 4 and 5](#), it can also be seen that these drugs bind to the same pocket in COX-1. This may infer that they could share a mechanism by reducing prostaglandin production, helping to control inflammation. However, this could also contribute to gastrointestinal side effects (ulcers, gastritis) and joint/bone inflammation (osteoporosis, joint pain).

3.2. Molecular dynamics

Molecular Dynamics (MD) simulations were conducted on the top-binding compounds to analyze their interactions. A dynamic model was constructed, particularly for proteins, where internal movements and conformational shifts can significantly influence their function (Hospital et al., 2015). To simulate these molecular trajectories, specialized algorithms were employed using a force field (FF) approach. There are two primary methods for MD simulations: (i) the atomistic model, which provides high accuracy and is typically applied to smaller systems, and (ii) the coarse-grained approach, where molecules are represented by ‘pseudo-atoms’ that approximate groups of atoms. While the atomistic method offers greater precision, the coarse-grained technique is preferred for metalloproteins due to the larger size of the system under study (Comba, 2003; Han et al., 2018; Hospital et al., 2015; Kmiecik et al., 2016).

In most cases, the ligands remain stable in the active center of the macromolecules. The best docking score of each ligand was selected for Molecular Dynamics.

In [Figure 7\(A\)](#), the Root Mean Square Deviation, RMSD, of azathioprine is presented over the 200 ns duration of the MD simulation, using its initial docking pose as the reference for measuring the RMSD of the ligand’s heavy atoms. Throughout the simulation, the ligand remains highly stable, with an RMSD value consistently below 4.0 Å, as shown in [Figure 7\(A\)](#).

In [Figure 7\(B\)](#), the RMSD of the protein’s C α atoms is shown remains below 6.0 Å, demonstrating good system convergence. The ligand’s RMSD over the 200 ns MD simulation is also shown, with the initial docking pose serving as the reference for measuring the heavy atoms’ RMSD. For most of the simulation, the ligand remains stable, maintaining an RMSD of approximately <6.0 Å, as depicted in [Figure 7\(B\)](#).

In [Figure 7\(C\)](#), the protein’s C α atoms are shown to exhibit an RMSD below 3.0 Å, further indicating good system convergence. Similarly, the ligand’s RMSD is tracked throughout the 200 ns simulation, using the initial docking pose as a reference for its heavy atoms. Throughout most of the simulation, the ligand remains stable, with an RMSD of approximately <6.0 Å, as illustrated in [Figure 7\(C\)](#).

3.3. Saturation transfer difference (STD)

After confirming the effectiveness of azathioprine in inhibiting 5-LOX, our objective was to explore its direct interactions and accurately identify the epitope involved in binding with 5-LOX. To investigate this interaction, we utilized Saturation Transfer Difference (STD) NMR, a technique that can evaluate a

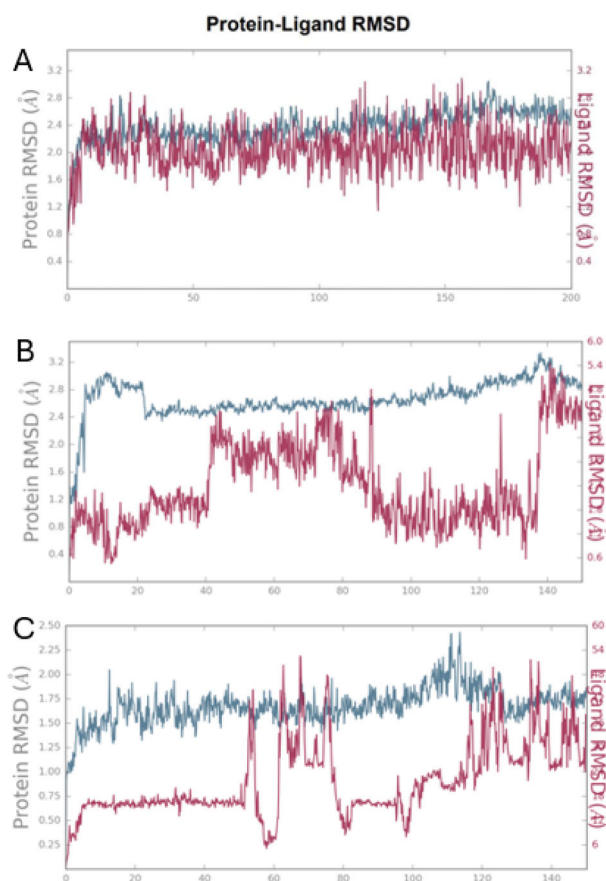


Figure 7. Azathioprine with 5-LOX display a RMSD value ($<4.0 \text{ \AA}$) (A). Prednisone with MAO-B display a RMSD value ($<6.0 \text{ \AA}$) (B). Pyridostigmine with carbonic anhydrase VII display a RMSD value ($<3.0 \text{ \AA}$) (C).

ligand's interaction with a pharmaceutical target and identify the specific protons involved in the binding process. The reason that azathioprine was chosen was because it is the most common drug for the treatment of Myasthenia Gravis.

The results of the STD NMR analysis illustrating the interaction between 5-LOX are shown in Figure 8. Analysis of the difference spectrum reveals that the peaks corresponding to the aromatic and aliphatic protons of azathioprine have decreased intensity compared to the reference ^1H -NMR spectrum. This finding confirms the interaction between azathioprine and 5-LOX. Furthermore, the comparison between the ^1H -NMR spectrum of the compound complex and the STD difference spectrum shows that all protons are involved in the protein's binding site. Specifically, the red spectrum (STD result) highlights ligand protons interacting with the protein, while the blue spectrum (initial proton NMR) shows all ligand protons as a reference. The reduced intensity of peaks in the STD difference spectrum, compared to the reference spectrum without the ligand, confirms the binding interaction. The chemical shifts (ppm) of azathioprine in the reference spectrum (blue) also remain unchanged in the STD spectrum (red), confirming no significant alteration in the electronic environment of the protons. Key peaks appear around δ 8.6, 7.8, and 3.5 ppm, corresponding to aromatic and aliphatic protons. The matching ppm values between spectra confirm structural stability, while the intensity changes in the red spectrum reveal which protons are involved in binding.

The NMR spectrum confirms the expected chemical shifts of azathioprine in the given buffer system. No unexpected peaks or significant peak shifts are observed, indicating the stability of azathioprine under these conditions.

An STD-NMR experiment was also performed to investigate the possible interaction between prednisone and 5-LOX enzyme in phosphate buffer at pH 7.2. Thus, we prepared an NMR tube solution containing 2.5 μL of prednisone (stock), 10 μL of 5-LOX, 50 μL of D_2O and 435.5 μL of phosphate buffer at pH = 7.15. The spectra were subsequently obtained, using a Bruker 500 MHz spectrometer of the Chemistry Department of the University of Athens.

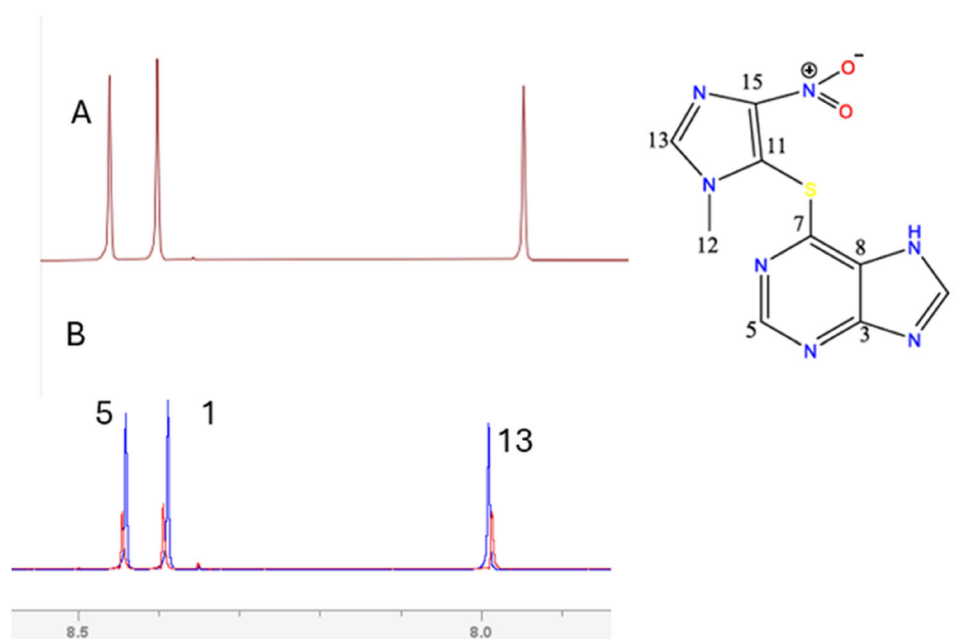


Figure 8. (A) Control experiment of azathioprine in buffer, (B) the STD difference spectrum, (red) The STD-NMR reference spectrum of azathioprine (20 mM) in the presence of 5-LOX protein (0.02 mM) at a 1:1000 ratio with respect to azathioprine, was obtained in potassium phosphate buffer at pH 7.2 and 600 μ L D₂O, using a 900 MHz NMR spectrometer at 25 °C (blue).

Table 3. Correlation of binding protons with their corresponding chemical shifts.

Atom number ¹ H	Chemical shift (ppm)	Peak multiplicity	Coupling constants (J, Hz)
H-1	7.76	d	10.6
H-2	6.21	d	12.2
H-4	6.12	s	–

s: singlet, d: doublet.

In this particular experiment, the difference spectrum demonstrated the presence of distinct signals at the following chemical shifts: 7.76 ppm for (H-1), 6.21 ppm for (H-2) and 6.12 ppm for (H-4), of prednisone. This fact demonstrates the existence of direct contact of the specific parts of the molecule with the enzyme binding cavity, thus providing clear evidence of prednisone binding to LOX-5, strongly underlining its role as a potential inhibitor and regulator of enzyme activity. The observed interaction sets the basis for further pharmacodynamic and structural investigation with advanced NMR spectroscopy and molecular modeling techniques.

The above results are provided in detail in Table 3, and the experimental STD spectrum is shown in Figure 9.

3.3.1. STD intensity (I_{STD}) calculation procedure

The calculation of the STD intensity (I_{STD}) was carried out according to the methodology described below.

Initially, using the Advanced Processing Options in the TopSpin software, the saturation spectrum was subtracted from the reference spectrum. The resulting data was processed based on the following equation:

$$I_{STD} = I_0 - I_{sat}/I_0$$

where I_0 represents the intensity of a given signal in the reference spectrum, and I_{sat} denotes the intensity of the corresponding signal in the saturation spectrum.

This calculation allows for the quantification of the signal attenuation due to saturation, thereby providing valuable information regarding the interaction between the ligand and the target within the framework of the STD-NMR technique.

The results of the analysis are presented in Table 4.

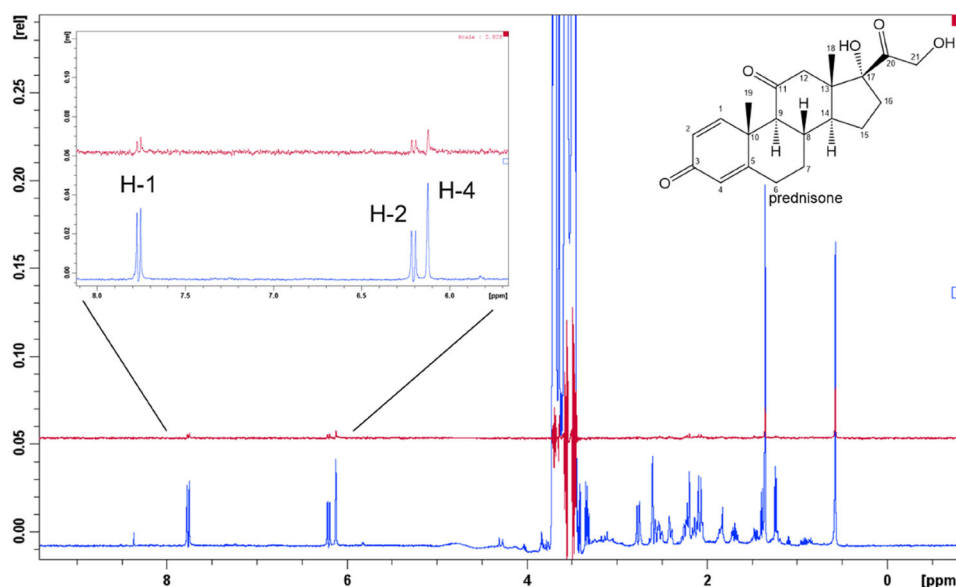


Figure 9. The blue graph (bottom) corresponds to the ^1H spectrum, of prednisone, in the presence of 5-Lox, in phosphate buffer with pH = 7.2. The red graph corresponds to the difference spectrum (STD), after the application of selective saturation.

Table 4. Results of STD NMR experiments of prednisone and azathioprine..

Prednisone			Azathioprine		
Atom number 1H	STD (%)	Residual(%)	Atom number 1H	STD (%)	Residual(%)
H-1	7.73	92.27	H-1	36.0	64.0
H-2	9.68	90.32	H-5	39.0	61.0
H-4	12.00	88.00	H-13	37.0	63.0

3.4. In vitro evaluation against human 15-LOX-1, LOX-1 and 5-LOX enzymes

Finally, we investigated the inhibitory potency of azathioprine and prednisone against human 15-LOX-1, LOX-1 and 5-LOX, which are isoenzymes of the LOX family. Our aim was to evaluate the selectivity profile of the compounds through an initial inhibitory screening to both enzymes at 100 μM . As shown in Figure 10(A), both azathioprine and prednisone significantly inhibited human 15-LOX-1, whereas no inhibition was observed for LOX-1 and 5-LOX. The inhibitory potency of these compounds, was confirmed by determination of their IC_{50} values, calculated as 133 μM and 112 μM for azathioprine and prednisone, respectively (Figure 10(B,C)).

3.5. ADMET results

The physicochemical parameters, ADME and toxicity results of pyridostigmine, azathioprine and prednisone according to preADMET.

According to preADMET, the BBB value for all the compounds is less than one, classifying them as inactive in the Central Nervous System (CNS). All the compounds exhibit high values for human intestinal absorption, suggesting they could be well absorbed from the intestinal tract when administered orally. Also, pyridostigmine and azathioprine are substrates to CYP_{3A4}, meaning that they are susceptible to interactions with drugs that affect this enzyme's activity. Furthermore, most of the compounds do not inhibit CP isoenzymes, indicating they are not toxic and do not produce unwanted adverse effects. Specifically, ADMET analysis revealed that several candidate compounds are substrates or inhibitors of major cytochrome P450 isoforms, including CYP_{3A4} and CYP_{2D6}. This has important implications for pharmacokinetics, as CYP450 enzymes play a central role in drug metabolism and clearance. Inhibition or induction of these enzymes could alter plasma drug concentrations, potentially leading to toxicity or therapeutic failure when co-administered with other drugs. Therefore, compounds that

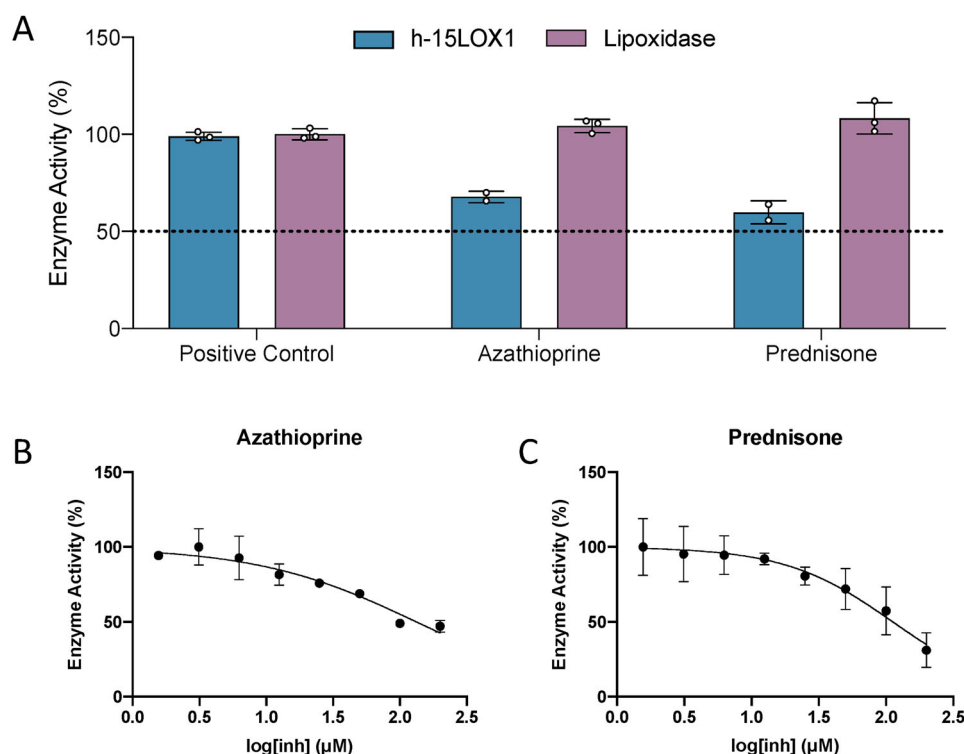


Figure 10. (A) Compounds tested (at 100 μM) against human 15-LOX-1, LOX-1 and 5-LOX enzymes. Positive control (absence of potential inhibitor) was set to 100% (dashed line = 50%). The averages and deviations of the individual measurements are presented. IC₅₀ plots of human 15-LOX-1 inhibition with (B) Azathioprine (IC₅₀ = 133 ± 50 μM) and (C) Prednisone (IC₅₀ = 112 ± 42 μM). The results are averages of triplicates, and the curves are derived by non-linear curve fitting. All the values are reported with the standard deviation after non-linear curve fitting. All experiments were performed in triplicate (*n* = 3), and the standard error is reported.

Table 5. The physicochemical parameters for compounds pyridostigmine, azathioprine and prednisone.

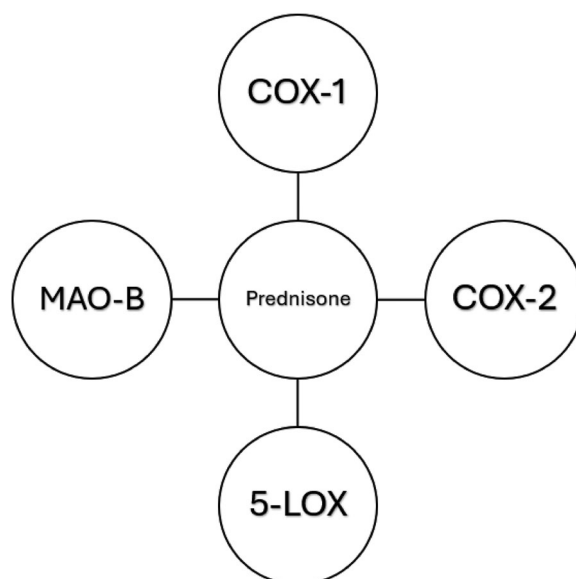
Properties	Pyridostigmine	Azathioprine	Prednisone
Molecular weight (g/mol)	181.215	277.269	358.434
Log P	0.5715	1.1458	1.7658
Rotatable bonds	1	3	2
Hydrogen Bond Acceptors	2	8	5
Hydrogen Bond Donors	0	1	2
Surface Area (Å ²)	77.356	109.818	91.67
Water solubility (log mol/L)	−0.389	−2.887	−3.899

Table 6. The ADME results of pyridostigmine, azathioprine and prednisone according to preADMET.

	Pyridostigmine	Azathioprine	Prednisone
BBB (log BB)	0.533942	0.118812	0.0282157
Buffer_solubility (mg/L)	4863.86	4455.41	10332.8
Caco2 (nm/sec)	39.8076	0.436158	17.7716
CYP_2C19_inhibition	None	None	None
CYP_2C9_inhibition	None	None	Inhibitor
CYP_2D6_inhibition	None	None	None
CYP_2D6_substrate	Weak	None	None
CYP_3A4_inhibition	None	None	Inhibitor
CYP_3A4_substrate	Substrate	Substrate	Weak
HIA (HIA %)	99.663672	75.504087	92.470856
MDCK (nm/sec)	1.14184	10.94	10.2951
Pgp_inhibition	None	None	None
Plasma_Protein_Binding (%)	0.000000	75.317930	63.508896
Pure_water_solubility (mg/L)	180099	77.0703	369.002
Skin_Permiability (logKp,cm/hour)	3.26883	−4.92195	−3.91345

Table 7. Toxicity results of pyridostigmine, azathioprine and prednisone according to pKCSm.

Properties	Pyridostigmine	Azathioprine	Prednisone
Toxicity			
AMES toxicity	No	Yes	Yes
Max. tolerated dose (human) (log mg/kg/day)	0.646	0.527	−0.368
Herg I inhibitor	No	No	No
Herg II inhibitor	No	No	No
Oral Rat Acute Toxicity (LD50) (mol/kg)	2.304	2.47	2.384
Oral Rat Chronic Toxicity (LOAEL) (log mg/kg_bw/day)	1.792	1.631	1.799
Hepatotoxicity	No	Yes	Yes
Skin Sensitization	Yes	No	No

**Figure 11.** Interaction network of prednisone with key molecular targets.

strongly inhibit or are extensively metabolized by CYP450 isoforms may require further optimization or monitoring in polypharmacy scenarios. These findings highlight the need for careful consideration of metabolic pathways during lead optimization to reduce the risk of adverse drug-drug interactions. Finally, the drugs obey Lipinski's Rule of Five (Benet et al., 2016) and due to low lipophilicity can easily be absorbed in the body (Georgiou et al., 2022, 2024).

With this compelling new mutational signature evidence, we believe it is now even more important for physicians prescribing azathioprine to be aware of the increased risk of cutaneous malignancy and to routinely provide appropriate educational and surveillance support to minimize this risk. Further research to optimize such risk reduction strategies is now urgently required (Leigh et al., 2019).

The toxicity data indicates varying safety profiles among the three compounds. Pyridostigmine shows no AMES toxicity, does not inhibit hERG channels and has a relatively high maximum tolerated dose (0.646), suggesting a favorable safety profile with low acute toxicity (LD50 values of 2.304) and no hepatotoxicity. Azathioprine and prednisone, however, are predicted to be mutagenic (AMES positive) and potentially hepatotoxic, with lower maximum tolerated doses (0.527 and −0.368, respectively). Despite acceptable acute toxicity levels (LD50 of 2.47 and 2.384), the potential risks associated with mutagenicity and hepatotoxicity in these compounds raise safety concerns that warrant further investigation.

According to data available in preADMET, no hERG II (human Ether-à-go-go-Related Gene) inhibition has been reported for azathioprine. In contrast, skin sensitization associated with pyridostigmine has been documented in earlier studies. Pyridostigmine bromide (PB), when delivered transdermally, may be a useful pretreatment for organophosphate poisoning. PB transdermal formulations were developed as this route has the potential to provide a more constant, prolonged, and therapeutically effective drug level in the body.

To evaluate safety, guinea pig skin sensitization studies were conducted using a variation of the split adjuvant technique with various PB transdermal formulations. Three gel matrix formulations were tested:

1. 50% PB
2. 30% PB with 0.198% sodium lauryl sulfate (SLS)
3. 30% PB with 0.21% of a proprietary surfactant (PS).

SLS and the proprietary surfactant were included as dermal penetration enhancers. Nine groups of 10 animals were induced and challenged with one of the three PB or PB/surfactant formulations (3 groups per formulation). Additionally, two groups of 10 animals were used as positive controls and were induced and challenged with 2,4-dinitrochlorobenzene (DNCB).

The results indicate that 44% of the animals responded positively to the 50% PB formulation at challenge, while 80% responded positively to the 30% PB/0.198% SLS formulation, and 82% responded to the 30% PB/0.21% PS formulation. This study demonstrates that PB is a potential contact sensitizer, with an enhanced response when surfactants are present (Harris & Maibach, 1989).

In a previous study using prednisone in *in vitro* models, Otsuka et al. reported no mutagenic activity based on the Ames test and mammalian cell gene mutation assay, though a slight increase in the incidence of structural chromosomal aberrations was observed (de Oliveira et al., 2021).

4. Conclusions

This research article focuses on three bioactive compounds azathioprine, prednisone and pyridostigmine, drugs used for the treatment of Myasthenia Gravis. STD NMR experiments confirmed the binding of azathioprine to LOX-5 at both the molecular and atomic levels. These findings are consistent with the proposed conformations derived from *in-silico* computational studies. *In-silico* experiments conducted on various macromolecules revealed that the compounds exhibited a strong binding affinity to many enzymes. Moreover, *in vitro* enzymatic evaluation showed that both azathioprine and prednisone inhibit human 15-LOX-1 at micromolar concentrations. This suggests low selectivity, which could potentially explain the compounds' broad pharmaceutical applications, particularly for prednisone.

However, this lack of selectivity may also be linked to the occurrence of side effects, as the compounds might interact with multiple targets within the body. Molecular Dynamics simulations indicated that all the molecules remain stable in the active centers. Additionally, all derivatives exhibit no hepatotoxicity and comply with Lipinski's Rule of Five, suggesting they are safe and bioactive. These findings imply their potential for various biological and pharmacological applications, such as CNS drugs. This research offers valuable insights for synthetic chemists interested in developing new structures, with the ultimate goal of utilizing *in silico* molecular modeling to synthesize molecules that selectively target certain biological entities.

The high binding energy of prednisone may be explained from its structural features. It is a rigid molecule with high lipophilic entry and hydrophobic segments. Its amphiphilic nature enables interactions with a wide range of biological targets and is MD stable for the most of the high binding poses (Figure 7). Azathioprine also acts on some targets also suggesting the possibility of being a more selective drug. This study aims to reveal possible novel targets for well-known drugs. The serendipity of the targets of the three molecules shows their possible wide pharmaceutical index but rings the danger bell of side effects. One of the major problems posed by the three drugs azathioprine, prednisone, and pyridostigmine is that although they are used for Myasthenia Gravis treatment, their beneficial effects are symptomatic. This triggered our interest in examining their selectivity, possibly to explain their pharmaceutical action and find new pharmaceutical uses for repurposing.

For implementing these aims we studied the molecular interactions of these three compounds with various enzyme targets. Using computational approaches like docking, molecular dynamics, and ADME analysis, alongside experimental NMR validation, we explored their binding to targets such as COX, MAO, angiotensin receptors, and LOX. The results reveal promising drug-like properties and minimal toxicity as expected, and potential broader applications, particularly as CNS therapeutics.

Author contributions

CRedit: **Errikos Petsas**: Conceptualization; **Eleftherios Massios**: Data curation; **Nikitas Georgiou**: Methodology; **Antigoni Cheilari**: Software; **Panagiotis Konstantinos Papadimitriou**: Resources; **Margarita Georgia Kakava**: Validation; **Ektoras Vasileios Apostolou**: Data curation; **Ioannis Angelonidis**: Data curation; **Nikolaos Eleftheriadis**: Investigation, Methodology; **Demeter Tzeli**: Investigation; **Thomas Mavromoustakos**: Investigation, Methodology.

Disclosure statement

No potential conflict of interest was reported by the authors.

Funding

This work benefited from access to University of Utrecht and has been supported by iNEXT-Discovery, project number PID: 25512, funded by the Horizon 2020 program of the European Commission. N.G. and D.T. acknowledge computational time granted by the Greek Research & Technology Network (GRNET) in the National HPC facility ARIS under project ID pr015035-TrMeCo.

ORCID

Demeter Tzeli  <http://orcid.org/0000-0003-0899-7282>

References

- Adamis, K. S., Georgoulakis, M., Angelonidis, I., Korovesis, D., Papadopoulos, C., Kapsalis, M., Tavernarakis, N., Eleftheriadis, N., & Neochoritis, C. G. (2025). The evolution of fluorescein into a potential theranostic tool. *Chemistry (Weinheim an Der Bergstrasse, Germany)*, 31(34), e202501513. <https://doi.org/10.1002/chem.202501513>
- Asada, H., Inoue, A., Ngako Kadji, F. M., Hirata, K., Shiimura, Y., Im, D., Shimamura, T., Nomura, N., Iwanari, H., Hamakubo, T., Kusano-Arai, O., Hisano, H., Uemura, T., Suno, C., Aoki, J., & Iwata, S. (2020). The crystal structure of angiotensin II type 2 receptor with endogenous peptide hormone. *Structure (London, England: 1993)*, 28(4), 418–425.e4. <https://doi.org/10.1016/j.str.2019.12.003>
- Barrett, D. G., Deaton, D. N., Hassell, A. M., McFadyen, R. B., Miller, A. B., Miller, L. R., Payne, J. A., Shewchuk, L. M., Willard, D. H., & Wright, L. L. (2005). Acyclic cyanamide-based inhibitors of cathepsin K. *Bioorganic & Medicinal Chemistry Letters*, 15(12), 3039–3043. <https://doi.org/10.1016/j.bmcl.2005.04.032>
- Benet, L. Z., Hosey, C. M., Ursu, O., & Oprea, T. I. (2016). BDDCS, the rule of 5 and drugability. *Advanced Drug Delivery Reviews*, 101, 89–98. <https://doi.org/10.1016/j.addr.2016.05.007>
- Benlloch, R., Shevela, D., Hainzl, T., Grundström, C., Shutova, T., Messinger, J., Samuelsson, G., & Elisabeth Sauer-Eriksson, A. (2015). Crystal structure and functional characterization of photosystem II-associated carbonic anhydrase CAH3 in chlamydomonas reinhardtii. *Plant Physiology*, 167(3), 950–962. <https://doi.org/10.1104/pp.114.253591>
- Buemi, M. R., Di Fiore, A., De Luca, L., Angeli, A., Mancuso, F., Ferro, S., Monti, S. M., Buonanno, M., Russo, E., De Sarro, G., De Simone, G., Supuran, C. T., & Gitto, R. (2019). Exploring structural properties of potent human carbonic anhydrase inhibitors bearing a 4-(cycloalkylamino-1-carbonyl)benzenesulfonamide moiety. *European Journal of Medicinal Chemistry*, 163, 443–452. <https://doi.org/10.1016/j.ejmech.2018.11.073>
- Chande, N., Townsend, C. M., Parker, C. E., & MacDonald, J. K. (2016). Azathioprine or 6-mercaptopurine for induction of remission in Crohn's disease. *The Cochrane Database of Systematic Reviews*, 10(10), CD000545. <https://doi.org/10.1002/14651858.CD000545.pub5>
- Cheung, J., Rudolph, M. J., Burshteyn, F., Cassidy, M. S., Gary, E. N., Love, J., Franklin, M. C., & Height, J. J. (2012). Structures of human acetylcholinesterase in complex with pharmacologically important ligands. *Journal of Medicinal Chemistry*, 55(22), 10282–10286. <https://doi.org/10.1021/jm300871x>
- Comba, P. (2003). Inorganic and bioinorganic molecular mechanics modeling—the problem of the force field parameterization. *Coordination Chemistry Reviews*, 238–239, 9–20. [https://doi.org/10.1016/S0010-8545\(02\)00286-2](https://doi.org/10.1016/S0010-8545(02)00286-2)
- de Oliveira, L. C., de Melo Bisneto, A. V., Puga, S. C., Fernandes, A. S., Vêras, J. H., Cardoso, C. G., Ribeiro e Silva, C., Carneiro, C. C., & Chen-Chen, L. (2021). Prednisone is genotoxic in mice and drosophila melanogaster. *Mutation Research. Genetic Toxicology and Environmental Mutagenesis*, 865, 503334. <https://doi.org/10.1016/j.mrgentox.2021.503334>
- Eleftheriadis, N., Neochoritis, C. G., Leus, N. G. J., van der Wouden, P. E., Dömling, A., & Dekker, F. J. (2015). Rational development of a potent 15-lipoxygenase-1 inhibitor with in vitro and ex vivo anti-inflammatory properties. *Journal of Medicinal Chemistry*, 58(19), 7850–7862. <https://doi.org/10.1021/acs.jmedchem.5b01121>

- Eleftheriadis, N., Poelman, H., Leus, N. G. J., Honrath, B., Neochoritis, C. G., Dolga, A., Dömling, A., & Dekker, F. J. (2016a). Design of a novel thiophene inhibitor of 15-lipoxygenase-1 with both anti-inflammatory and neuroprotective properties. *European Journal of Medicinal Chemistry*, 122, 786–801. <https://doi.org/10.1016/j.ejmech.2016.07.010>
- Eleftheriadis, N., Thee, S. A., Zwinderman, M. R. H., Leus, N. G. J., & Dekker, F. J. (2016b). Activity-based probes for 15-lipoxygenase-1. *Angewandte Chemie International Edition*, 55(40), 12300–12305. <https://doi.org/10.1002/anie.201606876>
- Essmann, U., Perera, L., Berkowitz, M. L., Darden, T., Lee, H., & Pedersen, L. G. (1995). A smooth particle mesh ewald method. *The Journal of Chemical Physics*, 103(19), 8577–8593. <https://doi.org/10.1063/1.470117>
- Georgiou, N., Goulени, N., Chontzopoulou, E., Skoufas, G. S., Gkionis, A., Tzeli, D., Vassiliou, S., & Mavromoustakos, T. (2023). Structure assignment, conformational properties and discovery of potential targets of the ugi cinnamic adduct NGI25. *Journal of Biomolecular Structure & Dynamics*, 41(4), 1253–1266. <https://doi.org/10.1080/07391102.2021.2017356>
- Georgiou, N., Karta, D., Cheilari, A., Merzel, F., Tzeli, D., & Vassiliou, S. (2024). Synthesis of thiazolidin-4-ones derivatives, evaluation of conformation in solution, theoretical isomerization reaction paths and discovery of potential biological targets. 1–20.
- Georgiou, N., Katsogiannou, A., Skourtis, D., Iatrou, H., Tzeli, D., Vassiliou, S., Javornik, U., Plavec, J., & Mavromoustakos, T. (2022). Conformational properties of new thiosemicarbazone and thiocarbohydrazone derivatives and their possible targets. *Molecules (Basel, Switzerland)*, 27(8), 2537. <https://doi.org/10.3390/molecules27082537>
- Gilbert, N. C., Bartlett, S. G., Waight, M. T., Neau, D. B., Boeglin, W. E., Brash, A. R., & Newcomer, M. E. (2011). The structure of human 5-lipoxygenase. *Science (New York, N.Y.)*, 331(6014), 217–219. <https://doi.org/10.1126/science.1197203>
- Glukhova, A., Thal, D. M., Nguyen, A. T., Vecchio, E. A., Jörg, M., Scammells, P. J., May, L. T., Sexton, P. M., & Christopoulos, A. (2017). Structure of the adenosine A1 receptor reveals the basis for subtype selectivity. *Cell*, 168(5), 867–877.e13. <https://doi.org/10.1016/j.cell.2017.01.042>
- Han, Y., Jin, J., Wagner, J. W., & Voth, G. A. (2018). Quantum theory of multiscale coarse-graining. *The Journal of Chemical Physics*, 148(10), 102335. <https://doi.org/10.1063/1.5010270>
- Harris, G. L., & Maibach, H. I. (1989). Allergic contact dermatitis potential of 3 pyridostigmine bromide transdermal drug delivery formulations. *Contact Dermatitis*, 21(3), 189–193. <https://doi.org/10.1111/j.1600-0536.1989.tb04734.x>
- Hospital, A., Goñi, J. R., Orozco, M., & Gelpi, J. L. (2015). Molecular dynamics simulations: Advances and applications. *Advances and Applications in Bioinformatics and Chemistry: AABC*, 8, 37–47. <https://doi.org/10.2147/AABC.S70333>
- Hua, T., Li, X., Wu, L., Iliopoulos-Tsoutsouvas, C., Wang, Y., Wu, M., Shen, L., Brust, C. A., Nikas, S. P., Song, F., Song, X., Yuan, S., Sun, Q., Wu, Y., Jiang, S., Grim, T. W., Benchama, O., Stahl, E. L., Zvonok, N., ... Liu, Z. J. (2020). Activation and signaling mechanism revealed by cannabinoid receptor-gi complex structures. *Cell*, 180(4), 655–665.e18. <https://doi.org/10.1016/j.cell.2020.01.008>
- Hua, T., Vemuri, K., Nikas, S. P., Laprairie, R. B., Wu, Y., Qu, L., Pu, M., Korde, A., Jiang, S., Ho, J. H., Han, G. W., Ding, K., Li, X., Liu, H., Hanson, M. A., Zhao, S., Bohn, L. M., Makriyannis, A., Stevens, R. C., & Liu, Z. J. (2017). Crystal structures of agonist-bound human cannabinoid receptor CB 1. *Nature*, 547(7664), 468–471. <https://doi.org/10.1038/nature23272>
- Humphreys, D. D., Friesner, R. A., & Berne, B. J. (1994). A multiple-time-step molecular dynamics algorithm for macromolecules. *The Journal of Physical Chemistry*, 98(27), 6885–6892. <https://doi.org/10.1021/j100078a035>
- Imtiaz, S., Muzaffar, S., & Ali, S. M. (2021). Demonstrating accuracy of the already proposed protocol for structure elucidation of cyclodextrin inclusion complexes by validation using quantitative ROESY analysis. *Journal of Inclusion Phenomena and Macrocyclic Chemistry*, 100(1–2), 71–87. <https://doi.org/10.1007/s10847-021-01047-9>
- Jin, Z., Du, X., Xu, Y., Deng, Y., Liu, M., Zhao, Y., Zhang, B., Li, X., Zhang, L., Peng, C., Duan, Y., Yu, J., Wang, L., Yang, K., Liu, F., Jiang, R., Yang, X., You, T., Liu, X., ... Yang, H. (2020). Structure of Mpro from SARS-CoV-2 and discovery of its inhibitors. *Nature*, 582(7811), 289–293. <https://doi.org/10.1038/s41586-020-2223-y>
- Jorgensen, W. L., Maxwell, D. S., & Tirado-Rives, J. (1996). Development and testing of the OPLS all-atom force field on conformational energetics and properties of organic liquids. *Journal of the American Chemical Society*, 118(45), 11225–11236. <https://doi.org/10.1021/ja9621760>
- Julian, L. D., Wang, Z., Bostick, T., Caille, S., Choi, R., DeGraffenreid, M., Di, Y., He, X., Hungate, R. W., Jaen, J. C., Liu, J., Monshouwer, M., McMinn, D., Rew, Y., Sudom, A., Sun, D., Tu, H., Ursu, S., Walker, N., ... Powers, J. P. (2008). Discovery of novel, potent benzamide inhibitors of 11 β -hydroxysteroid dehydrogenase type 1 (11 β -HSD1) exhibiting oral activity in an enzyme inhibition ex vivo model. *Journal of Medicinal Chemistry*, 51(13), 3953–3960. <https://doi.org/10.1021/jm800310g>
- Kim, E. E., & Wyckoff, H. W. (1991). Reaction mechanism of alkaline phosphatase based on crystal structures. *Journal of Molecular Biology*, 218(2), 449–464. [https://doi.org/10.1016/0022-2836\(91\)90724-k](https://doi.org/10.1016/0022-2836(91)90724-k)
- Kmiecik, S., Gront, D., Kolinski, M., Wieteska, L., Dawid, A. E., & Kolinski, A. (2016). Coarse-grained protein models and their applications. *Chemical Reviews*, 116(14), 7898–7936. <https://doi.org/10.1021/acs.chemrev.6b00163>
- Košak, U., Brus, B., Knez, D., Šink, R., Žakelj, S., Trontelj, J., Pišlar, A., Šlenc, J., Gobec, M., Živin, M., Tratnjek, L., Perše, M., Safat, K., Podkova, A., Filipek, B., Nachon, F., Brazzolotto, X., Więckowska, A., Malawska, B., ... Gobec, S.

- (2016). Development of an in-vivo active reversible butyrylcholinesterase inhibitor. *Scientific Reports*, 6(1), 39495. <https://doi.org/10.1038/srep39495>
- Leigh, I. M., Proby, C. M., Inman, G. J., & Harwood, C. A. (2019). Azathioprine: Friend or foe? *The British Journal of Dermatology*, 180(5), 961–963. <https://doi.org/10.1111/bjd.17345>
- Louka, A., Spacho, N., Korovesis, D., Adamis, K., Papadopoulos, C., Kalaitzaki, E., Tavernarakis, N., Neochoritis, C. G., & Eleftheriadis, N. (2025). Crafting molecular tools for 15-lipoxygenase-1 in a single step. *Angewandte Chemie (International Ed. in English)*, 64(6), e202418291. <https://doi.org/10.1002/anie.202418291>
- Lyman, E., & Zuckerman, D. M. (2006). Ensemble-based convergence analysis of biomolecular trajectories. *Biophysical Journal*, 91(1), 164–172. <https://doi.org/10.1529/biophysj.106.082941>
- Martyna, G. J., Tobias, D. J., & Klein, M. L. (1994). Constant pressure molecular dynamics algorithms. *The Journal of Chemical Physics*, 101(5), 4177–4189. <https://doi.org/10.1063/1.467468>
- Offenbacher, A. R., Hu, S., Poss, E. M., Carr, C. A. M., Scouras, A. D., Prigozhin, D. M., Iavarone, A. T., Palla, A., Alber, T., Fraser, J. S., & Klinman, J. P. (2017). Hydrogen–deuterium exchange of lipoxygenase uncovers a relationship between distal, solvent exposed protein motions and the thermal activation barrier for catalytic proton-coupled electron tunneling. *ACS Central Science*, 3(6), 570–579. <https://doi.org/10.1021/acscentsci.7b00142>
- Papaemmanouil, C., Chatziathanasiadou, M. V., Chatzigiannis, C., Chontzopoulou, E., Mavromoustakos, T., Grdadolnik, S. G., & Tzakos, A. G. (2020). Unveiling the interaction profile of rosmarinic acid and its bioactive substructures with serum albumin. *Journal of Enzyme Inhibition and Medicinal Chemistry*, 35(1), 786–804. <https://doi.org/10.1080/14756366.2020.1740923>
- Pasinetti, G. M. (1996). Inflammatory mechanisms in neurodegeneration and alzheimer's disease: The role of the complement system. *Neurobiology of Aging*, 17(5), 707–716. [https://doi.org/10.1016/0197-4580\(96\)00113-3](https://doi.org/10.1016/0197-4580(96)00113-3)
- Reis, J., Manzella, N., Cagide, F., Miallet-Perez, J., Uriarte, E., Parini, A., Borges, F., & Binda, C. (2018). Tight-binding inhibition of human monoamine oxidase b by chromone analogs: A kinetic, crystallographic, and biological analysis. *Journal of Medicinal Chemistry*, 61(9), 4203–4212. <https://doi.org/10.1021/acs.jmedchem.8b00357>
- Samara, N. L., & Yang, W. (2018). Cation trafficking propels RNA hydrolysis. *Nature Structural & Molecular Biology*, 25(8), 715–721. <https://doi.org/10.1038/s41594-018-0099-4>
- Schacke, H. (2002). Mechanisms involved in the side effects of glucocorticoids. *Pharmacology & Therapeutics*, 96(1), 23–43. [https://doi.org/10.1016/S0163-7258\(02\)00297-8](https://doi.org/10.1016/S0163-7258(02)00297-8)
- Schrodinger. (2013). L.L.C. MacroModel. Version 10.
- Smith, W. L., DeWitt, D. L., & Garavito, R. M. (2000). Cyclooxygenases: Structural, cellular, and molecular biology. *Annual Review of Biochemistry*, 69(1), 145–182. <https://doi.org/10.1146/annurev.biochem.69.1.145>
- Son, S.-Y., Ma, J., Kondou, Y., Yoshimura, M., Yamashita, E., & Tsukihara, T. (2008). Structure of human monoamine oxidase A at 2.2-Å resolution: The control of opening the entry for substrates/inhibitors. *Proceedings of the National Academy of Sciences of the United States of America*, 105(15), 5739–5744. <https://doi.org/10.1073/pnas.0710626105>
- Spacho, N., Casertano, M., Imperatore, C., Papadopoulos, C., Menna, M., & Eleftheriadis, N. (2024). Investigating the catalytic site of human 15-lipoxygenase-1 via marine natural products. *Chemistry—A European Journal*, 30(53). <https://doi.org/10.1002/chem.202402279>
- Timm, J., Bosch-Navarrete, C., Recio, E., Nettleship, J. E., Rada, H., González-Pacanowska, D., & Wilson, K. S. (2015). Structural and kinetic characterization of thymidine kinase from leishmania major. *PLOS Neglected Tropical Diseases*, 9(5), e0003781. <https://doi.org/10.1371/journal.pntd.0003781>
- Version, D.D. Version, D. D. Desmond Tutorial. Schroedinger. https://doi.org/10.1162/rest_a_00790
- Viegas, A., Manso, J., Nobrega, F. L., & Cabrita, E. J. (2011). Saturation-transfer difference (STD) NMR: A simple and fast method for ligand screening and characterization of protein binding. *Journal of Chemical Education*, 88(7), 990–994. <https://doi.org/10.1021/ed101169t>
- Vrontaki, E., Leonis, G., Avramopoulos, A., Papadopoulos, M. G., Simčič, M., Grdadolnik, S. G., Afantitis, A., Melagraki, G., Hadjikakou, S. K., & Mavromoustakos, T. (2015). Stability and binding effects of silver(I) complexes at lipoxygenase-1. *Journal of Enzyme Inhibition and Medicinal Chemistry*, 30(4), 539–549. <https://doi.org/10.3109/14756366.2014.951348>
- Wang, J. L., Limburg, D., Graneto, M. J., Springer, J., Hamper, J. R. B., Liao, S., Pawlitz, J. L., Kurumbail, R. G., Maziasz, T., Talley, J. J., Kiefer, J. R., & Carter, J. (2010). The novel benzopyran class of selective cyclooxygenase-2 inhibitors. Part 2: The second clinical candidate having a shorter and favorable human half-life. *Bioorganic & Medicinal Chemistry Letters*, 20(23), 7159–7163. <https://doi.org/10.1016/j.bmcl.2010.07.054>
- Whittington, D. A., Waheed, A., Ulmasov, B., Shah, G. N., Grubb, J. H., Sly, W. S., & Christianson, D. W. (2001). Crystal structure of the dimeric extracellular domain of human carbonic anhydrase XII, a bitopic membrane protein over-expressed in certain cancer tumor cells. *Proceedings of the National Academy of Sciences of the United States of America*, 98(17), 9545–9550. <https://doi.org/10.1073/pnas.161301298>